

Prospects for detecting charged long-lived BSM particles at MoEDAL-MAPP experiment: A mini-review

Rafał Maselek^{1*} and Kazuki Sakurai²

^{1*}Theoretical Physics Department, Jožef Stefan Institute, Jamova cesta 39, Ljubljana, 1000, Slovenia.

²Institute of Theoretical Physics, Faculty of Physics, University of Warsaw, Pasteura 5, Warsaw, 02-093, Poland.

*Corresponding author(s). E-mail(s): rafal.maselek@ijs.si;
Contributing authors: kazuki.sakurai@fuw.edu.pl;

Abstract

The search for physics beyond the Standard Model at the Large Hadron Collider is expanding to include unconventional signatures such as long-lived particles. This mini-review assesses the prospects for detecting electrically charged long-lived particles using the MoEDAL-MAPP experiment. We synthesize findings from recent studies that evaluate sensitivity to supersymmetric models, radiative neutrino mass scenarios, and generic multiply charged objects. A key component of this review is the comparative analysis of MoEDAL's reach against the general-purpose ATLAS and CMS experiments. We conclude that while MoEDAL is constrained by lower integrated luminosity, its passive, background-free detection methodology offers a unique advantage. Specifically, the experiment provides complementarity to the major detectors, particularly for signals involving slow-moving particles and stable states with intermediate electric charges.

Keywords: High Energy Physics, MoEDAL-MAPP, Beyond the Standard Model, Long Lived Particles

1 Introduction

The Standard Model (SM) of particle physics, despite its remarkable success, leaves several fundamental questions unanswered, such as the nature of dark matter, the origin of neutrino masses, and the hierarchy problem. Many theoretical frameworks proposed to address these shortcomings—including Supersymmetry (SUSY), universal extra dimensions, and various hidden sector models—predict the existence of new massive particles. While the majority of searches at the Large Hadron Collider (LHC) focus on prompt decays, a significant subset of these Beyond the Standard Model (BSM) theories naturally gives rise to Long-Lived Particles (LLPs) that can travel appreciable distances through the detectors before decaying [1].

The search for charged LLPs has become a key frontier at the LHC. The general-purpose detectors, ATLAS and CMS, have deployed extensive search programs targeting Heavy Stable Charged Particles (HSCPs) and multi-charged objects. These analyses typically exploit anomalous ionisation energy loss (dE/dx) in the inner trackers and Time-of-Flight (ToF) measurements in the muon systems to identify slow-moving, heavy candidates. Recently, the ATLAS collaboration published results using the full Run 2 dataset (139 fb^{-1}), placing stringent limit on meta-stable gluino R-hadrons, $m \gtrsim 2 \text{ TeV}$ [2], as well as multi-charged particles ($|q| \geq 2e$) up to the TeV range [3]. Similarly, the CMS collaboration has published its updated HSCP search using the Run 2 data (101 fb^{-1}), excluding gluino R-hadrons with masses up to $\sim 2 \text{ TeV}$ and identifying exclusion limit for a doubly charged fermion $\gtrsim 1.4 \text{ TeV}$ [4].

Despite these impressive constraints, general-purpose detectors face intrinsic limitations. They rely heavily on specific triggers, often requiring high transverse momentum (p_T) or missing energy, which can be inefficient for slow-moving ($\beta \ll 1$) or non-standard signal topologies. Furthermore, standard detector electronics may saturate when exposed to the extreme ionization densities produced by highly charged objects ($|q| \gg 1e$), potentially leading to signal loss.

The MoEDAL experiment is able to cover some of these blind spots. MoEDAL employs passive Nuclear Track Detectors (NTDs) and Magnetic Monopole Trappers (MMTs) that are sensitive to highly ionizing particles without the need for electronic triggers or precise timing [5]. This allows for the detection of particles with arbitrarily low velocities and very high electric or magnetic charges, a regime often inaccessible to ATLAS and CMS. Specifically, the MoEDAL collaboration has searched for Highly Electrically Charged Objects (HECOs) with $|q| \geq 10e$ using Run 1 [6] and Run 2 [7] data.

In preparation for LHC Run 3, the experiment has been upgraded to MoEDAL-MAPP. While the new MAPP subdetector extends sensitivity to neutral, feebly interacting particles, the core program for charged LLPs remains centred on the enhanced NTD arrays. This mini-review synthesizes a series of phenomenological studies that evaluate the detector's potential. We discuss discovery prospects for charged LLPs arising from SUSY, neutrino mass models, and generic highly charged scenarios, highlighting the regions of parameter space where MoEDAL-MAPP provides unique, background-free sensitivity complementary to the major LHC experiments.

2 MoEDAL-MAPP experiment

The **Monopole and Exotics Detector at the LHC** (MoEDAL) is a small, mostly passive LHC detector located about 2 m away from the IP8, outside of the LHCb VELO detector. It was designed mainly to discover magnetic monopoles [5], but its search programme includes dyons, Q-balls, black hole remnants, and highly ionising massive particles. MoEDAL comprises of the three main subdetector systems: Nuclear Track Detectors (NTDs), Magnetic Monopole Trappers (MMTs), and TimePix (TPX).

The main subsystem consists of an array of over a hundred NTD panels, each measuring 25 cm in width and length, and only a couple of millimetres in depth. Each panel consists of 6 layers of special polymer, which degrade when penetrated by a highly ionising particle. NTD is a passive detector system; after a long exposure, the NTD array is dismantled and transported to an external laboratory, where panels are disassembled, and each polymer layer is etched with a special solvent. The etching dissolves the outer layer of the polymer, but along the energy deposition, the speed of dissolving is larger. As a result, cone-shaped etch pits are formed on both sides of the NTD panels, revealing the trajectory of ionising particles. By analysing the shapes and alignment of etch pits in 6 layers of an NTD panel, the presence of a signal can be established. The key properties of this method are: 1) the expected SM background is $\ll 1$, making it a background-free experiment; 2) the possibility to reconstruct a track depends on the particle's velocity, charge, and incidence angle. The NTD array is the main detector used in searches for charged long-lived particles that are the topic of this article.

The other detector subsystem is MMT, designed to capture magnetic monopoles for later examination, and a pixel detector, TPX, for real-time monitoring of the radiative environment. In preparation for the Run 3 data taking period, MoEDAL has been augmented with a **MoEDAL Apparatus for Penetrating Particles (MAPP)**, a scintillator detector for discovery of Feebly Interacting Particles. The collaboration decided on changing its name and has been using "MoEDAL-MAPP" since then.

3 Methodology of phenomenological studies

In the following part of the article, we discuss a series of phenomenological studies aimed at assessing the discovery potential for various charged long-lived BSM particles at the MoEDAL-MAPP experiment. In contrast to the major LHC experiments, such as ATLAS and CMS, no public simulation framework suitable for these signatures was available. To address this gap, a dedicated fast-simulation framework in PYTHON has been developed. The code focuses on modelling the Nuclear Track Detector array of MoEDAL, as it is the only detector subsystem relevant for the charged long-lived particles considered in this work.

The code accepts LHE files with simulated BSM events as its input. For each event, the final state particles are identified, and their four-momenta are extracted. Next, the locations and dimensions of the NTD panels are loaded from the Run 2 MoEDAL geometry file (see Fig. 1). Particle trajectories are checked for intersecting the NTD array, with a set of simplifying assumptions in mind. First, the particles are assumed to propagate between their creation and the detector without significant loss

of energy or change in momentum. The possibility of a decay is handled by assigning weights to particles at a later stage of the analysis. Moreover, the depth of the NTD panels is neglected, since it is three orders of magnitude smaller than the width and height. Particles whose trajectories do not intersect with NTD panels are rejected. The rest are subjected to velocity and incident angle constraints, as described in detail in [8]. The partial efficiency of particle i with charge Q , three-momentum \vec{p}_i , velocity β_i , incidence angle δ_i , and lifetime τ_i is given by:

$$\epsilon_i = P_{\text{NTD}}(\vec{p}_i, \tau_i) \cdot \Theta(\delta_{\text{max}}(\beta_i, Q) - \delta_i,) \quad (1)$$

where $P_{\text{NTD}}(\vec{p}_i, \tau_i)$ is a probability of reaching the detector, Θ is the Heavyside step function, and $\delta_{\text{max}}(\beta_i, Q)$ is the maximum incidence angle for particle with velocity β_i and charge Q , above which it cannot be reconstructed. For Run 3, the NTD panels of the MoEDAL detector have been rearranged to face the interaction point, greatly leveraging the efficiency. For such detector placement, the Eq. (1) can be approximated with:

$$\epsilon_i = P_{\text{NTD}}(\vec{p}_i, \tau_i) \cdot \Theta(0.15 \cdot |Q| - \beta_i). \quad (2)$$

Eq. (2) reveals a crucial property of the MoEDAL detector: singly-charged particles have to be slow in order to be detectable at MoEDAL, in contrast to major LHC experiments like ATLAS and CMS, which are sensitive only for highly boosted particles. However, the velocity threshold grows for particles with larger electric charges leading to enhanced sensitivity, in principle, for $|Q| = 6\frac{2}{3}$, the velocity constraint becomes irrelevant.

The mean efficiency of the NTD panel array is calculated by summing over all partial efficiencies and averaging over the Monte Carlo sample:

$$\epsilon = \left\langle \sum_{i=1}^N \epsilon_i \right\rangle_{\text{MC}} = \left\langle \sum_{i=1}^N P_{\text{NTD}}(\vec{p}_i, \tau_i) \cdot \Theta(\delta_{\text{max}}(\beta_i, Q) - \delta_i,) \right\rangle_{\text{MC}}, \quad (3)$$

where we have used ϵ_i defined by Eq. (1). In Eq. (3), N is the number of BSM particles in an event, usually $N = 2$. The expected number of signal events that MoEDAL will detect over a period of data taking is:

$$N_{\text{sig}} = \sigma(m) \times L \times \epsilon, \quad (4)$$

where $\sigma(m)$ is the production cross-section of charged long-lived particles with mass m and L is the integrated luminosity.

4 Future discovery prospects

4.1 Proof-of-concept: neutralinos decaying to meta-stable staus

Although the possibility of searching for charged long-lived BSM particles at MoEDAL was foreseen in the experiment's technical design report [5], the first detailed assessment of MoEDAL's sensitivity has been presented in Ref. [9]. For the needs of this

MoEDAL detector

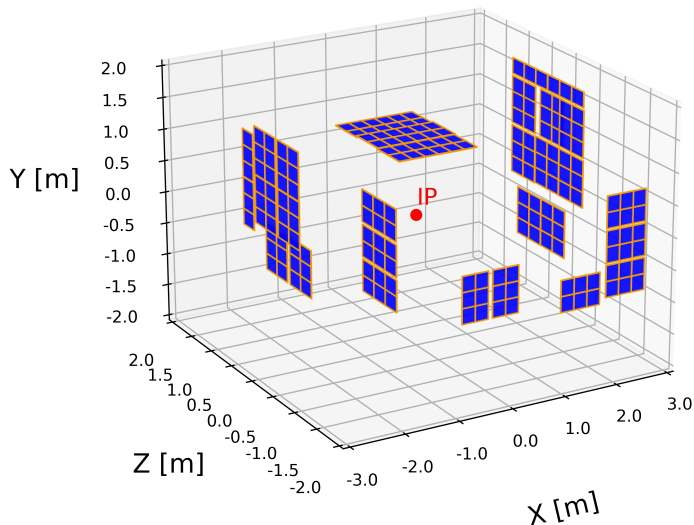


Figure 1: Nuclear Track Detector panel placement for the MoEDAL Run 2 geometry. Image taken from [8].

pioneering study, the fast simulation framework described in Sec. 3 was created. In this study, an interesting simplified supersymmetric model was introduced. In this model, a pair of gluinos is produced, each gluino decays promptly to two quarks and a long-lived neutralino, which subsequently decays to an off-shell tau and a metastable stau. The neutralino is assumed to be 30 GeV lighter than the gluino, in order to make the jets from gluino decay soft. A small mass splitting between neutralino and stau is assumed, 1 GeV, to ensure that the neutralino is long-lived. Since we are interested in the interaction of a stau with the MoEDAL detector, we assume staus are meta-stable (stable within the detector volume) without specifying its decay modes. Such suppressed stau decays can be realised, for example, via small RPV coupling to tau and other SM particles or, in a supergravity scenario, via Planck suppressed coupling to tau and gravitino.

This rather peculiar model possesses several features which make it attractive to study in MoEDAL. Firstly, gluinos are coloured particles with a relatively large production cross-section. Secondly, they are fermions, and fermions produced in the Drell-Yan process do not suffer from a p-wave suppression, unlike scalar particles. Thanks to that, their velocity distribution is shifted towards smaller values compared to e.g. staus, as can be seen in Fig. 2. Thirdly, the neutralino is promptly produced but meta-stable, leading to decreased efficiency in ATLAS and CMS detectors. Its long lifetime is advantageous for MoEDAL, but NTD panels can detect only highly ionising particles; therefore, decay to long-lived staus is necessary. The proposed model constitutes an optimal scenario from the MoEDAL's point of view. It possesses features

enhancing MoEDAL's efficiency and reducing the sensitivity of major LHC experiments. Therefore, it is a good benchmark to test if MoEDAL can compete with ATLAS and CMS.

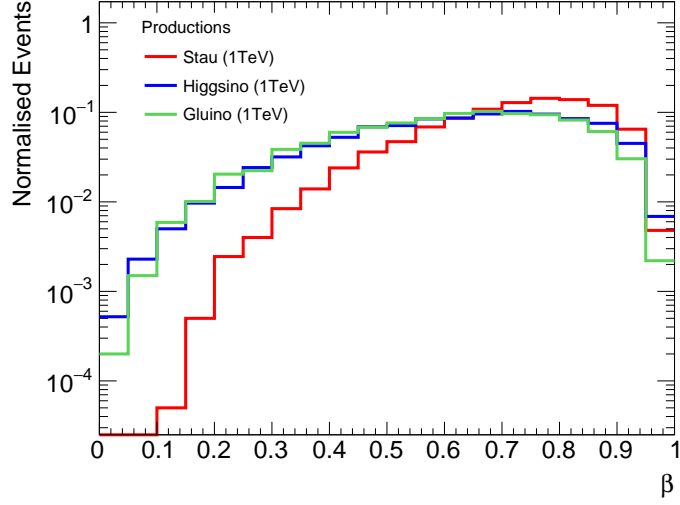


Figure 2: Velocity distributions for 1 TeV staus, Higgsinos, and gluinos produced via Drell-Yan process. Plot taken from [9].

For the considered scenario, the probability that a stau hits an NTD array is given by:

$$P_{\text{NTD}}(\vec{p}_{\tilde{\chi}_1^0}, \tau_{\tilde{\chi}_1^0}) = \omega(\vec{p}_{\tilde{\chi}_1^0}) \left[1 - \exp\left(-\frac{L_{\text{NTD}}(\vec{p}_{\tilde{\chi}_1^0})}{\beta\gamma c\tau_{\tilde{\chi}_1^0}}\right) \right], \quad (5)$$

where $\vec{p}_{\tilde{\chi}_1^0}$ and $\tau_{\tilde{\chi}_1^0}$ are neutralino's momentum and lifetime, respectively, L_{NTD} is the distance from IP to NTD panel along the neutralino's trajectory, β is particle's velocity, γ is Lorent factor, and $\omega(\vec{p}_{\tilde{\chi}_1^0})$ is either 1 or 0 depending on whether the particle's trajectory crosses the NTD array or not. The factor in the square-bracket corresponds to the probability that the neutralino decay $\tilde{\chi}_1^0 \rightarrow \tilde{\tau}\tau^*$ occurs before $\tilde{\chi}_1^0$ reaches an NTD. Due to the small mass splitting between the neutralino and the stau, we assume the momenta of the two particles are very similar.

In the study, we consider two scenarios. The first one is to take the Run 2 geometry and calculate efficiencies with Eq. (1). The second scenario, which we label "ideal", is to assume a slight rearrangement of NTD panels such that they face the IP directly. This allows us to neglect the impact of the incidence angle and use an approximation in Eq. (2).

The expected sensitivity of MoEDAL at the end of Run 3 ($L = 30 \text{ fb}^{-1}$) for the considered SUSY scenario is depicted in Fig. 3, where exclusion contours on gluino mass and neutralino's $c\tau$ are shown, assuming detection of $N_{\text{sig}} = 1$ (solid) or $N_{\text{sig}} = 2$

(dashed). The exclusion achievable with Run 2 geometry is depicted in red, while the sensitivity of the rearranged detector placement is shown in blue. One can see that the "ideal" geometry offers much better sensitivity, allowing for testing gluino masses up to 1.7 (1.55) TeV compared to 1.35 (1.2) TeV for Run 2 geometry when $N_{\text{sig}} = 1$ ($N_{\text{sig}} = 2$). In order to provide a comparison with major LHC experiments, we recast the ATLAS search for Heavy Stable Charged Objects [10], and depict it in Fig. 3 as a yellow contour. We scale the ATLAS constraint up to Run 3 luminosity ($L = 300 \text{ fb}^{-1}$) and depict it in orange. Interestingly, the character of the ATLAS constraint is different from MoEDAL's, and the latter offers better sensitivity for a broad range of neutralino decay lengths, when the "ideal" geometry set-up is used. This means that MoEDAL is able to provide not only independent, but also competitive constraints on some of the BSM Physics models. Results of this study lead to MoEDAL-MAPP collaboration's decision to rearrange NTD panels for Run 3, to match the "ideal" set-up.

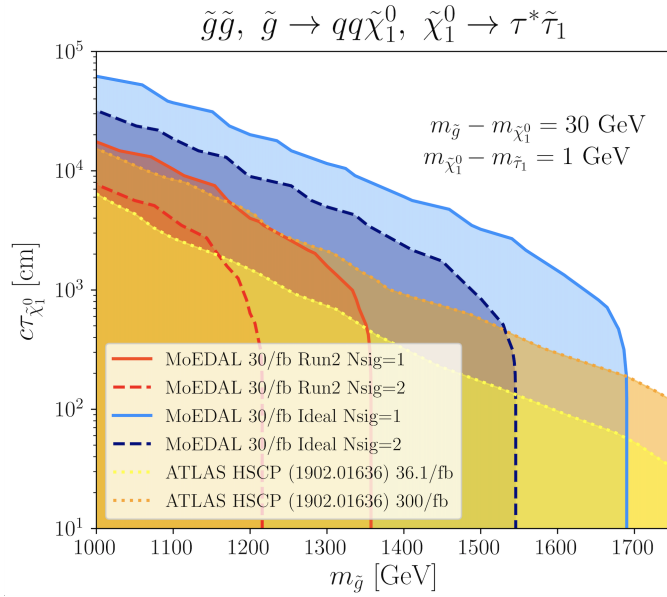


Figure 3: Expected sensitivity of the MoEDAL experiment to supersymmetric model. Red and blue contours correspond to Run 2 and "ideal" MoEDAL geometries, respectively. Solid line marks contours for $N_{\text{sig}} = 1$, while dashed lines are for $N_{\text{sig}} = 2$. The yellow contour shows constraints from ATLAS search for HSCPs [10], done for $L = 36.1 \text{ fb}^{-1}$. The orange contour is ATLAS constraint projected for the end of the Run 3 data taking period, $L = 300 \text{ fb}^{-1}$. Plot taken from [9].

4.2 Searches for supersymmetric long-lived particles

Encouraged by the promising results described in Sec. 4.1, a comprehensive evaluation of MoEDAL's performance for more typical BSM scenarios has been carried out in Ref. [11]. In this study, the pair production of supersymmetric particles was investigated, i.e. long-lived staus, charginos (wino- and Higgsino-like), and R-hadrons formed from gluinos, stops or light-flavour squarks.

A simple phenomenological description of R-hadron formation was adopted, assuming that R-hadrons are formed by supersymmetric particles together with up or down quarks. The possible bound states involving gluino are $\tilde{g}u\bar{u}$, $\tilde{g}d\bar{d}$, $\tilde{g}u\bar{d}$, and $\tilde{g}d\bar{u}$. The former two bound states are electrically neutral, hence they cannot be detected by MoEDAL. We introduce a free parameter, κ , representing a fraction of charged states amongst all produced R-hadrons, and vary it between 0.3 and 0.7.

For squarks, we consider two scenarios. First, we investigate the possibility when stops are relatively light compared to other squark flavours. In the second scenario, stops are heavy, and the other five flavours are nearly mass degenerate. In both cases, we assume that heavy squarks decay to the lightest one on a time scale $\ll \mathcal{O}(1 \text{ m}/c)$. The lightest squark forms bound states with u and d quarks: $\tilde{u}\bar{u}$, $\tilde{d}\bar{d}$, $\tilde{u}\bar{d}$, $\tilde{d}\bar{u}$. Similarly to gluino R-hadrons, only a fraction κ of the final states are electrically charged.

In addition to supersymmetry, we also consider simplified scenarios featuring doubly charged particles, motivated by seesaw and left-right symmetric models. Our approach relies on a minimal set of assumptions: the particles are pair-produced through the Drell-Yan process, carry electric charge $\pm 2e$, and are either scalar or spin-1/2 fermionic fields. They are singlets under $SU(3)_C$ and transform either as singlets or triplets under $SU(2)_L$.

To calculate the expected sensitivity of MoEDAL at the end of Run 3 ($L = 30 \text{ fb}^{-1}$), the simulation framework was adjusted to accommodate new types of particles. In particular, the probability of reaching the NTD panel was:

$$P_{\text{NTD}}(\vec{p}, \tau) = \omega(\vec{p}) \exp\left(-\frac{L_{\text{NTD}}(\vec{p})}{\beta\gamma c\tau}\right). \quad (6)$$

From now on, the effect of the incidence angle is being neglected, which corresponds to the "ideal" geometry set-up described in Sec. 4.1.

The results of the study [11], for $N_{\text{sig}} = 1$ and $\kappa = 0.7$, are summarised in Tab. 1 and Tab. 2, together with constraints from ATLAS and CMS. For supersymmetric particles, ATLAS constraints for \tilde{g} , \tilde{t} , \tilde{W} , and $\tilde{\tau}$ were directly taken from HSCP search [10] with $L = 36.1 \text{ fb}^{-1}$. Although ATLAS in [10] did not interpret its results for light-flavour squarks or Higgsinos, we were able to obtain limits on these sparticles by recasting cross-section upper limits for Winos and sbottoms. The CMS constraints for gluinos, stops, and staus come from an analysis [12] based on a smaller data set, $L = 2.5 \text{ fb}^{-1}$. The same analysis provides limits on doubly-charged $SU(2)_L$ -singlet spin-1/2 fermions. With additional recasting, we were able to obtain limits on scalars and fermionic triplets.

The results in Tab. 1 and Tab. 2 show that, in most scenarios, MoEDAL cannot match the sensitivity achieved by ATLAS or CMS. There are, however, two notable

Table 1: Expected MoEDAL’s sensitivity to long-lived supersymmetric particles at the end of Run 3 ($L = 30 \text{ fb}^{-1}$) compared with ATLAS and CMS constraints (in parentheses). Constraints for squarks and Higgsinos (in double parentheses) were obtained by recasting results from Ref. [10]. Table taken from [11].

	MoEDAL	(ATLAS)	(CMS)
\tilde{g}	1600	(2000)	(1500)
\tilde{q}	1920	((2310))	-
\tilde{t}	920	(1350)	(1000)
\tilde{W}	670	(1090)	-
\tilde{h}	530	((1170))	-
$\tilde{\tau}$	61	(430)	(230)

Table 2: Expected MoEDAL’s sensitivity to long-lived doubly-charged particles at the end of Run 3 ($L = 30 \text{ fb}^{-1}$) compared with CMS constraints for singlet fermions (in parentheses) from Ref. [12] and reinterpreted results (in double parentheses) for other types of particles. Table taken from [11].

	MoEDAL	(CMS)
Scalar singlet	160	((320))
Fermion singlet	650	(680)
Scalar triplet	340	((590))
Fermion triplet	1130	((900))

exceptions. For the fermionic singlet, MoEDAL and CMS provide comparable sensitivity. For the fermionic $SU(2)_L$ triplet, MoEDAL is expected to outperform CMS by roughly 230 GeV. It is important to emphasise, though, that the CMS limits were obtained using a relatively small data set of only $L = 2.5 \text{ fb}^{-1}$.

MoEDAL’s generally lower sensitivity compared with the major LHC experiments can be traced to two main factors. First, due to the LHCb experiment’s operational constraints, MoEDAL, which shares the same interaction point, has access to roughly an order of magnitude less luminosity. Second, MoEDAL is only sensitive to slowly moving particles. Most particles produced at the LHC are ultrarelativistic unless they are very heavy, but such heavy states typically have small production cross sections; the reduced luminosity further suppresses MoEDAL’s reach in these cases. The relatively strong performance observed for doubly charged fermions arises from their enhanced ionisation power as well as the more favourable velocity spectrum of spin-1/2 particles produced via the Drell–Yan mechanism.

4.3 Testing radiative neutrino mass models

Neutrino oscillations constitute clear evidence for the BSM physics, since this phenomenon can occur only if neutrinos are massive, contrary to Standard Model predictions. It bears no surprise that many theoretical new physics models concentrate on explaining neutrino masses. One of such models has been proposed in Ref. [13], where neutrino masses are generated at the 1-loop level. The model introduces several new fields, including scalar $SU(2)_L$ singlet, S_1 , and triplet, S_3 , and three pairs of vector-like spin-1/2 fermions $(F_i \bar{F}_i) (i = 1, 2, 3)$ in $SU(2)_L$ doublet representations. The hypercharge assignment is 2, 3, 5/2, and $-5/2$ for S_1 , S_3 , F_i , and \bar{F}_i , respectively.

The Lagrangian of the model is given by:

$$\begin{aligned}
\mathcal{L}_{\text{BSM}} = & \mathcal{L}_{\text{KIN}} - \left[(h_{ee})_{ij} (e_R^i)^C (e_R^j)^C S_1^\dagger + (h_F)_{ij} L_i F_j S_1^\dagger + (h_{\bar{F}})_{ij} L_i \bar{F}_j S_3^\dagger + \text{h.c.} \right] + \\
& + \lambda_2 |H|^2 |S_1|^2 + \lambda_{3a} |H|^2 |S_3|^2 - \left[\lambda_5 H H S_1 S_3^\dagger + \text{h.c.} \right] + \\
& + \lambda_4 |S_1|^4 + \lambda_{6a} |S_3^\dagger S_3|^2 + \lambda_{6b} |S_3 S_3^\dagger S_3^\dagger S_3| + \lambda_7 |S_1|^2 |S_3|^2.
\end{aligned} \tag{7}$$

The experimental constraints on neutrino masses require that the product of λ_5 and $h_F h_{\bar{F}}$ couplings is small.

The feature of this model most relevant for MoEDAL is the presence of multiply charged mass eigenstates arising from the triplet scalar field, namely $S^{\pm 4}$, $S^{\pm 3}$, and $S^{\pm 2}$. These states are naturally long-lived provided that neither λ_5 nor the product $h_F h_{\bar{F}}$ is large. This makes the model testable at MoEDAL, and a dedicated study of this possibility has been presented in Ref. [14].

Ref. [14] contains prospects to test the model described by Eq. (7), including a comprehensive investigation of the impact of various couplings on the final sensitivity. In addition, a coloured version of the model is discussed in Ref. [14], which is obtained by promoting new scalar and fermionic fields to (anti-)triplets under $SU(3)_C$, and shifting their hypercharges by $-2/3$. In this article, we constrain ourselves to presenting the expected sensitivity of MoEDAL to multiply charged long-lived particles in separation from the original model. In other words, we treated masses and lifetimes of particles as free parameters, and we considered only particle-antiparticle pair creation¹. We used Eq. (6) when calculating MoEDAL's sensitivity. Unlike previous studies described in Sec. 4.1 and Sec. 4.2, we included additional production modes via photon-fusion, which we find non-negligible. This resulted in improved limits compared to Tab. 2 for doubly charged scalars.

Tab. 3 summarises MoEDAL's expected sensitivity to colour-singlet long-lived scalars and fermions. Results are shown for both Run 3 ($L = 30 \text{ fb}^{-1}$) and HL-LHC ($L = 300 \text{ fb}^{-1}$), and for $N_{\text{sig}} = 1$ and $N_{\text{sig}} = 3$. To compare MoEDAL's prospects for BSM detection with those of the major LHC experiments, we used limits from the ATLAS search for heavy long-lived multi-charged particles [15], based on $L = 36 \text{ fb}^{-1}$. In that study, the collaboration interpreted their results only for spin-1/2 fermions. We therefore estimated the corresponding limits for scalars by taking the cross-section bounds from [15] and assuming that the efficiencies are not strongly dependent on spin. For Run 3, the only projection available at the time of writing was for fermions [16], with an estimated reach of about 1500 GeV.

The conclusion from Tab. 3 is that, by the end of Run 3, MoEDAL is expected to provide weaker sensitivity to the considered BSM particles than the current constraints from the major LHC experiments, even when requiring only a single detected particle. At the end of the HL-LHC, MoEDAL's sensitivity to $S^{\pm 2}$ would remain below the ATLAS limit obtained with $L = 36 \text{ fb}^{-1}$. However, for $S^{\pm 3}$ and $S^{\pm 4}$, MoEDAL would exceed that sensitivity. For $F^{\pm 3}$, MoEDAL's HL-LHC reach would be slightly better than the ATLAS projection for the end of Run 3, but only if we use $N_{\text{sig}} = 1$ to set

¹In the full model, mixed production is possible, e.g. $S^{3+} \text{Sec.}$ can be produced together with S^{2-} via s-channel W boson exchange.

Table 3: Model-independent mass limits on long-lived multiply charged colour-singlet BSM particles. The first column contains limits for fermions from Ref. [15] for $L = 36 \text{ fb}^{-1}$, and our recast for scalar particles (in double parentheses). The second column contains the projection for fermions for Run 3 $L = 300 \text{ fb}^{-1}$, taken from [16]. The last two columns contain the expected sensitivity of MoEDAL for $L = 30 \text{ fb}^{-1}$ and $L = 300 \text{ fb}^{-1}$, respectively, for $N_{\text{sig}} = 3$ ($N_{\text{sig}} = 1$). All numbers are in GeV. Table taken from [14].

	current HSCP bound (36 fb^{-1})	HSCP (Run 3) (300 fb^{-1})	MoEDAL (Run 3) (30 fb^{-1})	MoEDAL (HL-LHC) (300 fb^{-1})
$S^{\pm 2}$	((650))	-	190 (290)	400 (600)
$S^{\pm 3}$	((780))	-	430 (610)	850 (1100)
$S^{\pm 4}$	((920))	-	700 (960)	1200 (1430)
$F^{\pm 3}$	1130	1500	800 (1030)	1300 (1550)

Table 4: Model-independent mass limits on long-lived multiply charged colour-(anti)triplet scalar particles. The first column contains limits (in double parentheses) estimated in Ref. [16], by scaling up 7 and 8 TeV CMS results [17] to 13 TeV and $L = 30 \text{ fb}^{-1}$. The second column contains projections at the end of Run 3 ($L = 300 \text{ fb}^{-1}$), taken from [16]. The last two columns contain the expected sensitivity of MoEDAL for $L = 30 \text{ fb}^{-1}$ and $L = 300 \text{ fb}^{-1}$, respectively, for $N_{\text{sig}} = 3$ ($N_{\text{sig}} = 1$). All numbers are in GeV. Table taken from [14].

	current HSCP bound (36 fb^{-1})	HSCP (Run 3) (300 fb^{-1})	MoEDAL (Run 3) (30 fb^{-1})	MoEDAL (HL-LHC) (300 fb^{-1})
$\tilde{S}^{\pm 4/3}$	((1450))	1700	880 (1050)	1250 (1400)
$\tilde{S}^{\pm 7/3}$	((1480))	1730	1080 (1250)	1450 (1650)
$\tilde{S}^{\pm 10/3}$	((1510))	1790	1200 (1400)	1600 (1800)

the limit. Overall, this indicates that while MoEDAL cannot compete with the major experiments in setting the strongest mass limits, its fundamentally different detection technique provides complementary and independent constraints.

Tab. 4 contains MoEDAL’s sensitivity to coloured scalars: $\tilde{S}^{\pm 4/3}$, $\tilde{S}^{\pm 7/3}$, and $\tilde{S}^{\pm 10/3}$. The limits are significantly stronger than the limits in Tab. 4, mainly due to larger production cross-sections. To compare MoEDAL’s discovery prospects with ATLAS and CMS, we again refer to Ref. [16], where 7 and 8 TeV CMS results [17] were rescaled to 13 TeV and $L = 36 \text{ fb}^{-1}$. Projections for Run 3 ($L = 300 \text{ fb}^{-1}$) were also taken from Ref. [16]. The result shown in Tab. 4 reveals that MoEDAL can offer a comparable sensitivity to ATLAS/CMS only for $\tilde{S}^{\pm 10/3}$ when both experiments use $L = 300 \text{ fb}^{-1}$ data set size. However, MoEDAL will collect this amount of data only at the end of the HL-LHC phase, while ATLAS and CMS will achieve it at the end of Run 3.

4.4 Searches for multiply charged BSM particles

The final paper in the series, Ref. [18], was focused on simplified BSM scenarios featuring multiply charged particles. The study considered both scalar and spin-1/2 fermionic states, taken either as singlets or triplets under $SU(3)_C$, with electric charges

spanning from $\pm 1e$ up to $\pm 8e$. All new fields were assumed to be $SU(2)_L$ singlets. In total, discovery prospects for 32 distinct classes of BSM particles at the LHC were systematically evaluated.

A special emphasis was put on an accurate production cross-section estimation. At the time of publication of Ref. [18], experimental searches for multiply charged BSM particles, e.g. [15], were assuming Drell-Yan production of BSM particles. While this is a justified assumption for particles with $q = \pm 1e$ or $q = \pm 2e$, it lead to significant underestimation of production cross-section for particles with larger electric charges, for which photon fusion (and gluon-photon fusion for coloured particles) becomes non-negligible.

To estimate discovery prospects for multiply charged long-lived BSM particles at the LHC, three search strategies were considered: (1) anomalous track searches (i.e. large dE/dx analyses) at CMS [12, 17] and ATLAS [10], (2) searches for charged LLPs at MoEDAL, (3) diphoton resonance searches [19]. The first two types of searches assume a production of a particle-antiparticle pair that propagates through the detector without decaying. The latter search strategy considers the formation of a bound state due to attractive electromagnetic and/or strong force, and its decay into a pair of photons, $pp \rightarrow \mathcal{B} \rightarrow \gamma\gamma$.

Fig. 4 contains the expected sensitivity of the three search strategies to 32 types of BSM LLPs studied. The results assume the integrated luminosity of 3 ab^{-1} for ATLAS/CMS and 300 fb^{-1} for MoEDAL, which corresponds to the end of the HL-LHC phase. Red curves represent the expected sensitivity of the large dE/dx searches, obtained by following the recasting procedure in Ref. [16] applied to the CMS results in Ref. [12]. These searches provide the strongest limits for particles with small electric charges, i.e. $|q| \leq 3e$. Their sensitivity slightly increases with the magnitude of the charge. Blue curves correspond to recasting the diphoton resonance searches by ATLAS in Ref. [19]. These searches provide no (or very weak) limits for particles with small electric charges, however, their sensitivity grows rapidly with the magnitude of charge, and makes them the most relevant for large charges, i.e. $|q| \geq 7e$. Finally, Fig. 4 contains three green curves (with uncertainty bands for coloured particles due to hadronisation) representing MoEDAL's sensitivity, calculated with Eq. (6), for $N_{\text{sig}} = 1, 2, 3$ particles detected. These limits grow with the magnitude of the electric charge. Interestingly, for intermediate charge magnitudes, i.e. $3e \leq |q| \leq 6e$, MoEDAL is able to provide better limits than major LHC experiments, despite ~ 10 lower luminosity. This is due to MoEDAL being background-free. For ATLAS and CMS, both background and signal scale up with increased luminosity, while for MoEDAL, only the signal grows; the background remains $\ll 1$. Finally, Fig. 4 provides a comparison with current experimental constraints by depicting them as grey-shaded areas.

5 Conclusions

Searches for charged long-lived BSM particles constitute a rapidly growing and interesting branch of collider studies. In this article, we have summarised prospects for detecting various kinds of charged LLPs in future years, focusing on the MoEDAL experiment. We have estimated MoEDAL's sensitivity to particles in the MSSM,

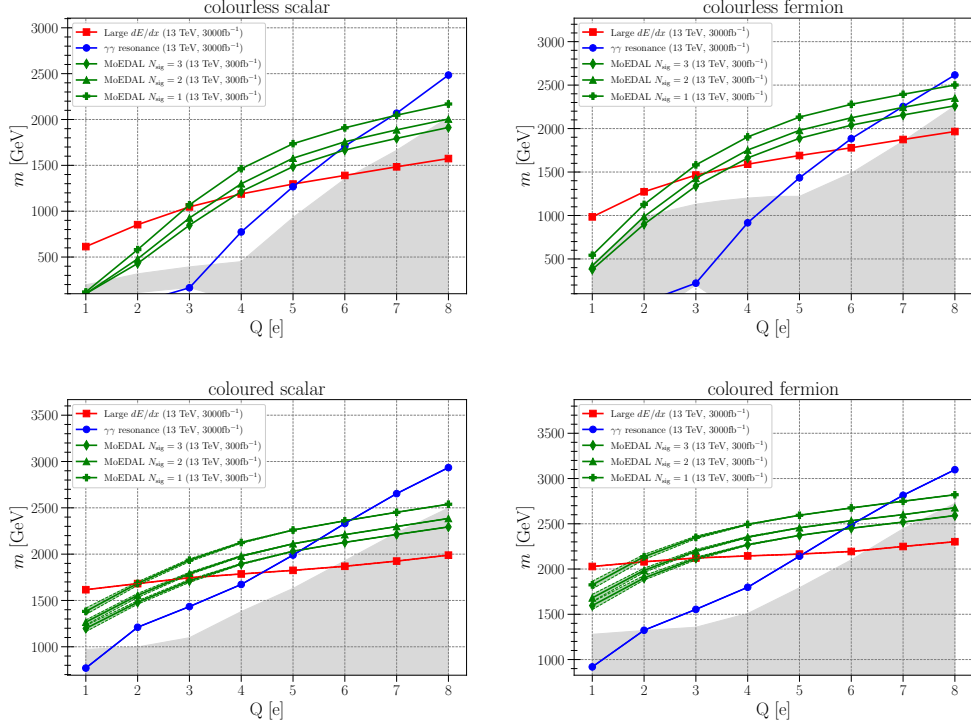


Figure 4: Expected sensitivity of LHC searches for multiply charged long-lived particles at the end of HL-LHC. Results are for colour-singlet scalars (top left), colour-singlet fermions (top right), colour-triplet scalars (bottom left), and colour-triplet fermions (bottom right). Figure taken from [18].

the radiative neutrino mass model, and various simplified models. We compared our findings to relevant constraints provided by ATLAS and CMS experiments.

We found that, in general scenarios with singly or doubly charged particles, MoEDAL offers lower sensitivity than major LHC experiments, mainly due to the lower luminosity available at the IP8. However, in some special cases, e.g. involving intermediate long-lived neutral particles like the one described in Sec. 4.1, MoEDAL can be more sensitive to new particles.

Due to its special detector design, MoEDAL achieves sensitivity comparable to ATLAS and CMS for particles with electric charges in the range $3e \lesssim |q| \lesssim 6e$. In the High-Luminosity LHC phase, MoEDAL is expected to be competitive with the general-purpose experiments, primarily due to its essentially background-free design.

Acknowledgements. This publication is co-funded by/ has received funding from/ the European Union’s Horizon Europe research and innovation program under the Marie Skłodowska-Curie COFUND Postdoctoral Programme grant agreement No.101081355-SMASH. The operation (SMASH project) is co-funded by the Republic of Slovenia and the European Union from the European Regional Development Fund.

Statement. Co-funded by the European Union. Views and opinions expressed are, however, those of the author(s) only and do not necessarily reflect those of the European Union or European Research Executive Agency. Neither the European Union nor the granting authority can be held responsible for them.

References

- [1] Alimena, J., *et al.*: Searching for long-lived particles beyond the Standard Model at the Large Hadron Collider. *J. Phys. G* **47**(9), 090501 (2020) <https://doi.org/10.1088/1361-6471/ab4574> [arXiv:1903.04497](https://arxiv.org/abs/1903.04497) [hep-ex]
- [2] Aad, G., *et al.*: Search for heavy, long-lived, charged particles with large ionisation energy loss in pp collisions at $\sqrt{s} = 13$ TeV using the ATLAS experiment and the full Run 2 dataset. *JHEP* **2306**, 158 (2023) [https://doi.org/10.1007/JHEP06\(2023\)158](https://doi.org/10.1007/JHEP06(2023)158) [arXiv:2205.06013](https://arxiv.org/abs/2205.06013) [hep-ex]
- [3] Aad, G., *et al.*: Search for heavy long-lived multi-charged particles in the full LHC Run 2 pp collision data at $s=13$ TeV using the ATLAS detector. *Phys. Lett. B* **847**, 138316 (2023) <https://doi.org/10.1016/j.physletb.2023.138316> [arXiv:2303.13613](https://arxiv.org/abs/2303.13613) [hep-ex]
- [4] Hayrapetyan, A., *et al.*: Search for heavy long-lived charged particles with large ionization energy loss in proton-proton collisions at $\sqrt{s} = 13$ TeV. *JHEP* **04**, 109 (2025) [https://doi.org/10.1007/JHEP04\(2025\)109](https://doi.org/10.1007/JHEP04(2025)109) [arXiv:2410.09164](https://arxiv.org/abs/2410.09164) [hep-ex]
- [5] Pinfeld, J., *et al.*: Technical Design Report of the MoEDAL Experiment. Technical report (June 2009). <https://inspirehep.net/files/ec50ce81fc2db37473c14c7a48a4e1b6>
- [6] Acharya, B., *et al.*: Search for highly-ionizing particles in pp collisions at the LHC's Run-1 using the prototype MoEDAL detector. *Eur. Phys. J. C* **82**(8), 694 (2022) <https://doi.org/10.1140/epjc/s10052-022-10608-2> [arXiv:2112.05806](https://arxiv.org/abs/2112.05806) [hep-ex]
- [7] Acharya, B., *et al.*: Search for Highly Ionizing Particles in pp Collisions during LHC Run 2 Using the Full MoEDAL Detector. *Phys. Rev. Lett.* **134**(7), 071802 (2025) <https://doi.org/10.1103/PhysRevLett.134.071802> [arXiv:2311.06509](https://arxiv.org/abs/2311.06509) [hep-ex]
- [8] Masełek, R.: Prospects for detecting long-lived particles at the Large Hadron Collider. PhD thesis, Warsaw U. (2023). <https://arxiv.org/abs/2310.13748>
- [9] Felea, D., Mamuzic, J., Masełek, R., Mavromatos, N.E., Mitsou, V.A., Pinfeld, J.L., Austri, R., Sakurai, K., Santra, A., Vives, O.: Prospects for discovering supersymmetric long-lived particles with MoEDAL. *Eur. Phys. J. C* **80**(5), 431 (2020) <https://doi.org/10.1140/epjc/s10052-020-7994-7> [arXiv:2001.05980](https://arxiv.org/abs/2001.05980) [hep-ph]

- [10] Aaboud, M., *et al.*: Search for heavy charged long-lived particles in the ATLAS detector in 36.1 fb^{-1} of proton-proton collision data at $\sqrt{s} = 13 \text{ TeV}$. Phys. Rev. D **99**(9), 092007 (2019) <https://doi.org/10.1103/PhysRevD.99.092007> [arXiv:1902.01636](https://arxiv.org/abs/1902.01636) [hep-ex]
- [11] Acharya, B.S., De Roeck, A., Ellis, J., Ghosh, D.K., Maselek, R., Panizzo, G., Pinfold, J.L., Sakurai, K., Shaa, A., Wall, A.: Prospects of searches for long-lived charged particles with MoEDAL. Eur. Phys. J. C **80**(6), 572 (2020) <https://doi.org/10.1140/epjc/s10052-020-8093-5> [arXiv:2004.11305](https://arxiv.org/abs/2004.11305) [hep-ph]
- [12] Khachatryan, V., *et al.*: Search for long-lived charged particles in proton-proton collisions at $\sqrt{s} = 13 \text{ TeV}$. Phys. Rev. D **94**(11), 112004 (2016) <https://doi.org/10.1103/PhysRevD.94.112004> [arXiv:1609.08382](https://arxiv.org/abs/1609.08382) [hep-ex]
- [13] R, C.A., Cottin, G., Helo, J.C., Hirsch, M.: Long-lived charged particles and multi-lepton signatures from neutrino mass models. Phys. Rev. D **101**(9), 095033 (2020) <https://doi.org/10.1103/PhysRevD.101.095033> [arXiv:2003.11494](https://arxiv.org/abs/2003.11494) [hep-ph]
- [14] Hirsch, M., Maselek, R., Sakurai, K.: Detecting long-lived multi-charged particles in neutrino mass models with MoEDAL. Eur. Phys. J. C **81**(8), 697 (2021) <https://doi.org/10.1140/epjc/s10052-021-09507-9> [arXiv:2103.05644](https://arxiv.org/abs/2103.05644) [hep-ph]. [Erratum: Eur.Phys.J.C 82, 774 (2022)]
- [15] Aaboud, M., *et al.*: Search for heavy long-lived multicharged particles in proton-proton collisions at $\sqrt{s} = 13 \text{ TeV}$ using the ATLAS detector. Phys. Rev. D **99**(5), 052003 (2019) <https://doi.org/10.1103/PhysRevD.99.052003> [arXiv:1812.03673](https://arxiv.org/abs/1812.03673) [hep-ex]
- [16] Jäger, S., Kvedaraitė, S., Perez, G., Savoray, I.: Bounds and prospects for stable multiply charged particles at the LHC. JHEP **04**, 041 (2019) [https://doi.org/10.1007/JHEP04\(2019\)041](https://doi.org/10.1007/JHEP04(2019)041) [arXiv:1812.03182](https://arxiv.org/abs/1812.03182) [hep-ph]
- [17] Chatrchyan, S., *et al.*: Searches for Long-Lived Charged Particles in pp Collisions at $\sqrt{s}=7$ and 8 TeV . JHEP **07**, 122 (2013) [https://doi.org/10.1007/JHEP07\(2013\)122](https://doi.org/10.1007/JHEP07(2013)122) [arXiv:1305.0491](https://arxiv.org/abs/1305.0491) [hep-ex]. [Erratum: JHEP 11, 149 (2022)]
- [18] Altakach, M.M., Lamba, P., Maselek, R., Mitsou, V.A., Sakurai, K.: Discovery prospects for long-lived multiply charged particles at the LHC. Eur. Phys. J. C **82**(9), 848 (2022) <https://doi.org/10.1140/epjc/s10052-022-10805-z> [arXiv:2204.03667](https://arxiv.org/abs/2204.03667) [hep-ph]
- [19] Aad, G., *et al.*: Search for resonances decaying into photon pairs in 139 fb^{-1} of pp collisions at $\sqrt{s}=13 \text{ TeV}$ with the ATLAS detector. Phys. Lett. B **822**, 136651 (2021) <https://doi.org/10.1016/j.physletb.2021.136651> [arXiv:2102.13405](https://arxiv.org/abs/2102.13405) [hep-ex]